ORIGINAL STUDY — KNEE

acta orthopaedica belgica, 2025, 91, 133-145

doi.org/10.52628/91.2.13582

Influencing factors in knee kinematics following posteriorly stabilized knee arthroplasty: a comprehensive analysis

L. STROOBANT[1], M. VERSTRAETE[1], S. VAN ONSEM[4], C. VAN DER STRAETEN[3], J. VICTOR[1], A. CHEVALIER[2]

[1]Department Orthopaedic Surgery, Ghent University Hospital, Gent, Belgium; [2]Department of Electromechanics, CosysLab and AnSyMo/Cosys Flandersmake, the strategic research center for the manufacturing industry, University of Antwerp, Antwerp, Belgium; 3Health Innovation and Research Institute, Ghent University Hospital, Ghent, Belgium; [4]Orthopaedics Department, AZ Alma Eeklo, Eeklo, Belgium.

Correspondence at: : Lenka Stroobant - Email: Lenkastroobant9@hotmail.com

Purpose: **Numerous papers present in-vivo knee kinematics data following total knee arthroplasty (TKA) from fluoroscopic testing. Comparing data is challenging given the large number of factors that could potentially affect the reported kinematics. This paper aims to understand the effects of some of the most pertinent factors:**

1. **What is the role of post-cam interaction and implant geometry in total knee kinematics?**
2. **Do tibiofemoral kinematics vary with different activities?**
3. **Is there a correlation between landmark-based and contact points kinematics?**

Methods: **Thirty patients who underwent TKA between 2014 and 2016 were assessed at a minimum follow-up period of six months. Given the use of three different posterior stabilized implants in the hospital, the first ten patients per implant who attended follow-up consultations and demonstrated a minimum of 90° knee flexion, were included in the study. The tibiofemoral kinematics during both open kinetic chain flexion-extension and closed kinetic chain exercises, such as rising from a chair and squatting, were examined using fluoroscopy. Single-plane fluoroscopic analysis (2D) was used to record the data, which was subsequently converted to 3D implant positions to evaluate the tibiofemoral contact points and landmark-based kinematic parameters.**

Results: **Significantly different anteroposterior translations and internal-external rotations were observed between the considered implants. Comparing the activities, a significantly more posterior position was observed for both the medial and lateral compartments in the closed chain activities during mid-flexion. A strong and significant correlation was found between the contact points and landmark-based analysis methods. However, large individual variations were also observed, yielding a difference of up to 25% in anteroposterior position between both methods.**

Conclusion: **In conclusion, all three evaluated factors significantly affect the obtained tibiofemoral kinematics.**

Level of Evidence: **Diagnostic, Level IV Case series**

Keywords: Knee kinematics, total knee arthroplasty, posterior-stabilized total knee prosthesis, fluoroscopy, post-cam engagement.

INTRODUCTION

Several research groups have already described in-vivo knee kinematics. However, a comparison of these studies is frequently challenging due to the substantial methodological variations observed across different studies[1–3]. Primarily, the implant type plays an important role in the kinematic pattern due to specific design properties. Consequently, conceptually similar implants can largely differ in their kinematics[4-7]. In addition, for the posteriorly stabilized design investigated in previous papers[4-7], the effect of post-cam engagement on kinematics remains unclear. Secondly, the observed kinematics are potentially influenced by muscle activity, as previously described by Victor and colleagues[8]. This highlights the importance of evaluating various activities during fluoroscopic assessment[9]. However, the extent to which this effect is consistent across different implants is uncertain.

Thirdly, the analytical method can also introduce differences in kinematics. Historically, the position of the femoral point nearest to the tibial tray has been used as reference for analyzing in-vivo knee kinematic[10,11]. However, this strategy does not consider the congruency between the insert and the femoral component. Alternatively, the analytical method

as outlined in the paper by Grood and Suntay uses anatomical landmarks to determine knee kinematics. This method is described in the guidelines provided by the International Society for Biomechanics (ISB) and is frequently advocated for ex-vivo testing[9]. However, there is a lack of knowledge regarding the relationship between the different analysis methods.

The purpose of this paper is to address the indicated lacunae in current knowledge by evaluating:

1. what the role is of post-cam interaction and implant geometry in total knee kinematics,
2. if tibiofemoral kinematics vary with different activities and
3. if there is a correlation between landmark-based and contact points kinematic analyses.

METHODS

Patient Population

The study was performed at Ghent University Hospital, Belgium. This study obtained approval from the Institutional Review Board (IRB) with the reference number B670201419601, along with informed consent from all participating patients.

A total of thirty TKA patients (10 male and 20 female) were included with a mean age of 63.9 years (SD 8.8) and a mean BMI of 27.1 kg/m² (SD 5.2). All had TKA performed between 2014 and 2016 for the preoperative diagnosis of osteoarthritis. The surgeries were performed by one of four senior knee surgeons (JV, NA, GVD, PD) utilizing a standardized, measured resection technique as outlined in a previous publication[12]. During this period, three different posterior-stabilized implant types were used for TKA. The first ten patients per implant, who attended follow-up consultations and were able to bend their knee at least 90°, were included in the study and received one the following implant types (Figure 1)[13]:

- Implant 1: anatomical multi-radius posterior stabilized design (Journey™ II Bi-Cruciate Stabilized knee system, Smith & Nephew, Memphis, TN, USA)
- Implant 2: single-radius posterior stabilized design (Unity™ knee system (Corin Ltd, Cirencester, UK)
- Implant 3: a size-optimized multi-radius posterior stabilized design (Persona® knee system, Zimmer-Biomet, Warsaw, IN, USA)

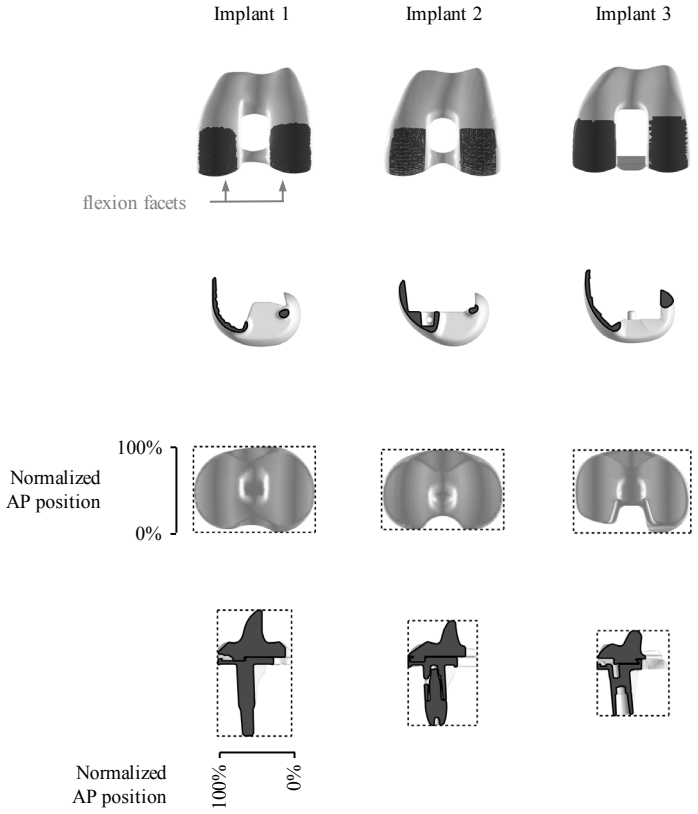

Fig. 1 — Geometry and orientation of implants studied in this paper with indication of normalized AP dimension on sagittal views for the tibial inserts.

Functional activity scoring of the patient's movements was performed using the Knee Injury and Osteoarthritis Outcome Score (KOOS) and Knee Society Score (KSS). The findings from this assessment were then correlated with the kinematic data, as reported in[13].

Test protocol

Sagittal plane images were captured at eight frames per second using a static fluoroscopy machine (Siemens Axion Luminos dRF)[13]. The patients performed three activities, covering both open and closed chain, weight bearing activities:

- FE: open chain flexion-extension movement against gravity, while seated on a chair.
- SQ: closed chain, unassisted squatting exercise from full extension to the maximum flexion possible and rising again.
- CH: rising from a chair and sitting back on the chair. The chair height was adjusted to the patient's height, resulting in a flexion angle of 90 degrees while seated.

All movements were repeated three times, and the case with the highest contrast images and widest captured range of motion was selected for analysis. Subsequently, the fluoroscopic videos were cropped into frames relevant to our study.

Using the 2D fluoroscopic images, a 3D reconstruction of the implants' position was subsequently determined by means of a validated 2D to 3D conversion technique (using the open source JointTrack software, University of Florida, Gainesville, FL, USA). In this method, computer-aided design (CAD) models are superimposed onto the fluoroscopic images using their silhouettes to derive transformation matrices of the CAD models within the image space. This yields an estimate of the position of the femoral component and tibial tray. This process was validated at our center and displayed errors below 0.6 degrees and 0.4 mm for all degrees of freedom except for the mediolateral translation[14]. The position of the polyethylene insert was derived from the position of the tray by matching their respective geometries, since we only considered fixed bearing implants. These positions were subsequently loaded in an in house-developed MATLAB (MathWorks Inc., MA, USA) program that calculated the tibiofemoral kinematics using both landmark-based and contact points methodologies.

The landmark-based methodology (GS) is based on the paper of Grood and Suntay[15]. An implant coordinate system associated with both prosthetic components was constructed based on tibial and femoral landmarks. The flexion facets of the femoral component were determined, and spherical shapes were fitted through both condyles. The medial and lateral centers of the spheres serve as reference points for describing mediolateral and anteroposterior translations. Dimensions perpendicular to the box geometry are used to describe the mediolateral and distal-proximal translations of the femoral component. The proximal-distal direction of the tibia is defined as normal to the tibial tray. Also, the anteroposterior and mediolateral directions were based on the geometric characteristics of the tray. In the anteroposterior position, the zero point is assigned to the most posterior location of the tibial tray. Based on these implant coordinate systems, a joint coordinate system was subsequently established. The mediolateral axis of the femur and the proximal-distal axis of the tibia were thereby used as the fixed axes. Afterwards, the translations were normalized using the maximum dimensions of the tibial tray in the corresponding direction (Figure 1)[15]. While all six degrees of freedom were assessed, this study primarily emphasizes the evaluation of the anteroposterior (AP) translation in both compartments of the knee and the internal-external (IE) rotation relative to the flexion angle. The rotation was determined based on the previously mentioned axes, specifically the angle between the mediolateral and anteroposterior axis.

In the contact points methodology (CP), the analyses were conducted using the implant's position (stl files) derived from the 2D to 3D conversion. First, a uniform mesh was selected with sufficiently small triangles (average edge length = 0.4 mm and triangle area = 0.07 mm²). Second, the contact points were determined utilizing the iterative closest point algorithm in MATLAB. This algorithm identifies the closest point from each surface A point to a point on surface B. The result is a heat mat, from which the contact points was defined as the center of gravity using the closest 200 mm² [16]. As in the GS-methodology, the AP translation was subsequently normalized (Figure 1).

The contact area can be calculated for each case. However, the resulting contact points locations were sometimes found to be widely dispersed. This was due to the inaccurate mediolateral position of single plane fluoroscopy[14]. As a result, the average implant position was calculated with respect to the overall AP and ML widths of the polyethylene insert. This resulted in %AP and %ML translations between 0 and 100%. This method allows for investigating the

kinematics of the implant for different implant sizes. Using these obtained positions, the contact points and post-cam engagements were determined. Here, post-cam engagement is defined as a distance smaller than 1 mm between the post and the cam.

To keep the overview, the subsequent sections of this paper will primarily focus on presenting the landmark-based results, unless explicitly indicated otherwise.

Statistical analysis

Statistics were conducted using IBM SPSS version 22 (IBM Corp., Chicago, IL, USA). A one-way ANOVA test with Bonferroni correction was used to evaluate the difference in kinematics for intervals of 10 degrees of flexion. This analysis was performed for the GS-method, comparing either different implants for a specific movement or different movements for a specific implant. The level of significance was set at 0.05 for all the statistical tests. To assess the correlation between the landmark-based and contact points methodologies, a Pearson correlation test and linear regression were used. In order to estimate the minimum required sample size, a power analysis was conducted using $\alpha = 0.05$ and effect size = 1.9, which was calculated based on the difference in anteroposterior translation in the lateral tibial component[17]. The analysis determined that a minimum group size of 7 was required to detect significant differences between the two groups with a power of 0.96. Therefore, a group size of 10 was selected for each implant type.

RESULTS

Mean kinematic patterns

An overview of the position (presented as mean and standard deviation) for the anteroposterior translation and internal-external rotation in the medial and lateral compartments for different degrees of flexion is described in Table I. Overall, the lateral compartment consistently exhibited a more posterior position in comparison to the medial compartment, independent of the implant type or activity.

Factor 1: Implant type

The following results are mainly described for the flexion-extension movement during the full range of motion. The results for the squatting exercise and the chair test are shown in Tables I and II.

Significant differences were observed among the different implants, particularly concerning the anteroposterior position of the medial condyle. For example, the medial condyle of implant 2 was positioned significantly more posteriorly compared to the other implants (Tables I and II). This applies to almost all movements and throughout the entire range of motion. Notably, throughout all movements in full extension, a significant more posteriorly positioned medial condyle of implant 3 was observed (Figure 2a). When comparing implants 1 and 3, a significantly more anterior position is described for implant 1 up to mid-flexion. However, beyond mid-flexion, both implants have a similar kinematic pattern, characterized by a posterior femoral rollback.

Regarding the lateral condyle, implants 1 and 2 showed a similar anteroposterior location during the entire range of motion (Figure 2b). A similar behavior was demonstrated for implant 3 in early to mid-flexion. Starting from mid-flexion (50°), implant 3 showed a significantly more anterior position compared to the other aforementioned implants.

For internal-external rotation, no significant differences were observed between implants 2 and 3 through the full range of motion. Implant 1 was more rotated externally during the entire range of motion compared to the other aforementioned implants, with a significant difference in full extension (implant 1 versus 3), 20 degrees of flexion and 110 degrees of flexion (implant 1 versus implant 2) (Figure 2c and Table 2). External rotation for implants 1 and 2 started with the unlocking of the knee between 0 and 10/20° (Figure 2c).

Besides the kinematic description, differences were observed between the implants in terms of post-cam engagement (Figure 3). The moment of engagement depended on the activity performed and the implant used. During the flexion-extension movement, implants 1 and 2 engaged first at 50 degrees of flexion, whereas implant 3 engaged at 70 degrees of flexion. Following the post-cam mechanism, a substantial posterior translation of both the medial and lateral condyles was observed across all the implants (Figure 2).

Factor 2: Activity type

Regarding the anteroposterior position of the medial and lateral condyles, the kinematic patterns for all the implants were similar during both closed-chain exercises (SQ and CH) (Table III). During the open chain flexion-extension in a sitting position, a more anterior position in the mid-flexion region was observed (Figure 4). This pattern is seen mainly in implants 1 and 3. In implant 2, the medial condyle was located significantly more posterior during squatting

Table I. — Overview of mean (SD) anteroposterior position and internal-external rotation through the range of motion for a given implant and activity. Results are displayed when available to more than 50% of the study population.

	Flexion	Implant 1			Implant 2			Implant 3		
	[degrees]	FE	SQ	CH	FE	SQ	CH	FE	SQ	CH
Medial AP translation [%]	-10						34.8 (3.6)			
	0	48.3 (2.3)		48.5 (2.4)	36.4 (1.6)	36.4 (2.8)	37.9 (4.8)	32.7 (2.4)	33.9 (4.0)	32.2 (3.2)
	10	50.6 (4.0)	53.6 (7.3)	50.2 (3.8)	37.6 (5.6)	35.7 (3.7)	38.2 (3.0)	39.2 (3.1)	41.8 (4.5)	40.2 (4.6)
	20	52.7 (4.3)	50.6 (5.1)	49.5 (4.9)	37.7 (4.0)	35.2 (4.2)	38.6 (2.7)	45.4 (3.8)	45.3 (3.4)	44.2 (3.2)
	30	54.8 (4.5)	50.7 (5.6)	48.8 (5.7)	40.2 (3.5)	35.4 (5.2)	38.9 (2.9)	48.4 (3.7)	45.6 (4.4)	45.5 (4.4)
	40	55.2 (4.3)	48.9 (4.6)	47.8 (5.2)	42.2 (3.3)	36.2 (3.4)	39.2 (3.6)	49.7 (4.1)	46.1 (4.9)	44.4 (5.3)
	50	54.0 (3.3)	47.6 (5.0)	47.1 (4.9)	43.2 (3.5)	37.4 (3.3)	39.7 (3.5)	50.6 (3.6)	45.3 (4.4)	44.6 (4.4)
	60	51.6 (2.8)	46.9 (3.9)	46.4 (4.1)	41.4 (3.8)	38.5 (3.7)	40.1 (3.0)	51.8 (4.2)	44.5 (4.0)	44.3 (4.9)
	70	48.5 (2.8)	46.1 (3.5)	46.2 (2.6)	37.9 (4.5)	36.7 (4.2)	39.2 (3.8)	52.4 (3.8)	42.9 (3.1)	44.0 (4.2)
	80	44.6 (3.8)	45.0 (2.4)	44.4 (1.6)	33.6 (4.0)	32.8 (2.9)	34.9 (3.9)	49.9 (3.0)	43.2 (2.7)	44.3 (2.8)
	90	40.4 (3.8)	41.0 (2.1)		29.8 (5.1)	29.6 (3.4)	27.1 (3.5)	45.0 (2.1)	42.5 (2.7)	
	100	35.9 (3.3)			25.0 (5.4)	23.8 (1.7)		39.5 (2.9)	38.5 (2.7)	
	110	31.8 (2.9)			20.8 (4.4)	18.6 (1.5)		33.2 (3.9)		
	120				18.3 (5.1)	12.5 (3.1)				
Lateral AP translation [%]	-10						37 (2.4)			
	0	42.9 (5.7)		43.6 (4.9)	37.5 (3.9)	39.2 (3.2)	39.3 (4.3)	35.4 (3.1)	33.8 (3.7)	35.8 (3.3)
	10	45.6 (7.6)	45.9 (11.3)	42.3 (7.2)	39.7 (4.2)	43.6 (9)	38.9 (4.0)	41.6 (2.2)	42.3 (4.2)	42.1 (2.4)
	20	47.1 (8.3)	42.2 (9.9)	40.5 (9.1)	40.6 (3.9)	41.6 (8.6)	38.2 (4.1)	47.5 (3.4)	46.4 (3.6)	46.1 (3.3)
	30	48.5 (8.9)	41.5 (8.5)	38.8 (9.3)	42.1 (4.3)	40.6 (7.6)	37.4 (4.3)	50.0 (4.8)	45.4 (3.3)	46.7 (4.9)
	40	47.7 (8.2)	38.2 (8.1)	36.8 (8.8)	43.4 (4.5)	40.4 (7.4)	37.4 (5.1)	50.1 (4.9)	45.5 (3.6)	44.0 (4.3)
	50	45.8 (6.6)	36.3 (6.9)	35.5 (7.8)	42.8 (4.5)	39.8 (6.6)	36.7 (4.9)	50.3 (4.1)	43.8 (3.3)	44.0 (4.7)
	60	43.4 (5.5)	34.7 (6.4)	34.3 (6.4)	40.3 (4.4)	39.3 (4.7)	36.5 (4.4)	49.7 (3.8)	43.0 (2.9)	42.7 (4.4)
	70	39.7 (4.0)	33.8 (6.0)	34.2 (3.7)	36.5 (4.3)	37.1 (4.0)	35.0 (4.2)	48.9 (3.9)	41.8 (2.3)	42.0 (3.8)
	80	35.0 (4.3)	31.6 (4.8)	34.6 (3.3)	32.0 (5.0)	32.7 (4.4)	30.5 (3.7)	45.4 (3.5)	41.6 (1.6)	40.7 (3.1)
	90	30.2 (4.6)	28.0 (5.5)		27.2 (4.8)	26.9 (4.8)	26.5 (3.8)	40.9 (3.0)	41.2 (1.4)	
	100	26.0 (4.6)			21.8 (4.7)	22.8 (5.0)		36.1 (2.8)	35.6 (2.3)	
	110	21.6 (4.6)			17.5 (4.9)	18.9 (6.0)		28.8 (3.5)		
	120				9.5 (3.2)	14.2 (6.5)				
Internal [>0] / external [<0] rotation [degrees]	-10	-0.6 (3.5)		-2.2 (3.4)	2.6 (1.2)	-1.6 (3.1)	1.6 (3.3)	1.1 (3.5)		1.6 (6.3)
	0	-4.2 (6.0)	-2.6 (1.0)	-3.9 (5.2)	1.1 (3.7)	3.3 (4.1)	2.0 (5.0)	2.4 (3.0)	3.6 (3.9)	3.2 (3.2)
	10	-3.5 (6.9)	-3.6 (6.9)	-5.9 (5.5)	1.8 (6.1)	5.3 (4.2)	2.4 (4.5)	2.3 (3.4)	2.3 (2.5)	2.1 (3.3)
	20	-4.3 (6.9)	-5.8 (6.3)	-6.4 (5.2)	2.3 (5.0)	4.1 (4.3)	1.5 (5.1)	2.0 (4.2)	2.6 (4.0)	2.1 (3.4)
	30	-4.5 (7.1)	-6.2 (6.7)	-7.3 (5.7)	1.1 (4.9)	3.0 (4.9)	-0.3 (4.6)	1.6 (4.3)	1.8 (4.4)	1.9 (3.3)
	40	-5.0 (6.3)	-7.7 (6.6)	-8.0 (5.6)	0.3 (5.2)	4.3 (7.4)	-0.8 (4.4)	0.6 (4.8)	1.2 (2.9)	0.6 (3.3)
	50	-5.8 (5.6)	-7.4 (7.2)	-8.6 (5.3)	-0.6 (5.1)	3.2 (7.0)	-2.2 (4.9)	-0.3 (4.1)	0.6 (2.1)	-0.1 (2.7)
	60	-6.4 (5.2)	-8.0 (6.0)	-8.8 (5.0)	-1.1 (5.4)	1.8 (6.0)	-3.3 (4.5)	-1.9 (4.1)	-0.1 (2.0)	-1.1 (2.7)
	70	-6.2 (5.5)	-8.1 (6.3)	-8.7 (3.6)	-1.3 (6.9)	1.9 (6.4)	-4.3 (5.2)	-2.7 (4.7)	0.0 (2.5)	-1.4 (2.5)
	80	-6.6 (6.6)	-8.9 (5.9)	-7.0 (3.1)	-1.6 (7.4)	1.6 (5.7)	-4.8 (5.2)	-3.5 (5.3)	0.2 (2.3)	-2.4 (2.8)
	90	-8.0 (7.7)	-8.5 (6.1)	-8.4 (5.1)	-2.1 (7.7)	0.1 (6.4)	-1.5 (5.7)	-2.4 (4.3)	0.8 (2.6)	-3.6 (2.3)
	100	-8.1 (5.8)	-5.1 (2.4)	-6.1 (1.6)	-2.2 (7.3)	1.9 (5.9)	-10.4 (0)	-1.8 (4.2)	-0.9 (2.8)	
	110	-6.9 (8.4)	-4.3 (1.5)		-2.3 (7.4)	3.0 (6.2)		-3.1 (5.4)	-3.3 (4.4)	
	120	-11.3 (5.5)			-7.0 (4.8)	3.3 (8.1)				

compared to flexion-extension between 30 and 50 degrees of flexion.

Internal-external rotation was similar for different performed activities, and applies uniformly to all implant types.

Significant disparities became apparent in the engagement of the post-cam mechanism across the performed activities. Notably, the engagement occurred earlier in the open chain exercise compared to the closed chain exercise involving weight bearing (Figure 3).

Factor 3: Analytical method

A comparison between the mean anteroposterior position, determined through the landmark-based method, and the position obtained from the contact

Table II. — Overview of the statistical difference in the anteroposterior position between the listed implants through the range of motion, shown for a given activity. The data are shown separately for the medial and the lateral compartments. The black values are indicative of a p-value less than 0.05.

degrees of flexion			0	10	20	30	40	50	60	70	80	90	100	110
medial AP movement	FE	Implant 1 - Implant 2	0,000	0,000	0,000	0,000	0,000	0,000	0,000	0,000	0,000	0,000	0,000	0,000
		Implant 1 - Implant 3	0,000	0,000	0,000	0,000	0,000	0,003	0,604	1,000	0,263	0,696	1,000	1,000
		Implant 2 - Implant 3	0,000	1,000	0,019	0,007	0,020	0,009	0,000	0,000	0,000	0,000	0,000	0,000
	SQ	Implant 1 - Implant 2	0,000	0,000	0,000	0,000	0,000	0,000	0,000	0,000	0,000	0,000	0,000	na
		Implant 1 - Implant 3	0,000	0,000	0,003	0,010	0,052	0,070	0,036	0,006	0,006	1,000	1,000	na
		Implant 2 - Implant 3	0,072	0,462	0,002	0,004	0,002	0,018	0,084	0,029	0,000	0,000	0,000	na
	CH	Implant 1 - Implant 2	0,000	0,000	0,000	0,000	0,001	0,002	0,005	0,000	0,000	0,000	na	na
		Implant 1 - Implant 3	0,000	0,000	0,000	0,026	0,035	0,050	0,067	0,024	0,420	0,851	na	na
		Implant 2 - Implant 3	0,000	1,000	0,186	0,132	0,624	0,598	0,931	0,400	0,000	0,000	na	na
lateral AP movement	FE	Implant 1 - Implant 2	0,145	0,060	0,051	0,099	0,386	0,611	0,443	0,254	0,434	0,429	0,114	0,219
		Implant 1 - Implant 3	0,001	0,033	1,000	1,000	1,000	1,000	0,200	0,002	0,001	0,001	0,001	0,192
		Implant 2 - Implant 3	0,283	1,000	0,267	0,189	0,371	0,109	0,006	0,000	0,000	0,000	0,000	0,004
	SQ	Implant 1 - Implant 2	0,001	1,000	1,000	1,000	1,000	0,443	0,085	0,193	0,844	1,000	1,000	na
		Implant 1 - Implant 3	0,000	0,578	1,000	1,000	0,350	0,189	0,036	0,024	0,000	0,000	0,011	na
		Implant 2 - Implant 3	0,009	1,000	1,000	1,000	1,000	1,000	1,000	1,000	0,005	0,000	0,001	na
	CH	Implant 1 - Implant 2	0,090	0,412	1,000	1,000	1,000	1,000	1,000	1,000	0,085	0,629	na	na
		Implant 1 - Implant 3	0,000	0,793	0,734	0,222	0,300	0,082	0,044	0,014	0,144	0,327	na	na
		Implant 2 - Implant 3	0,019	1,000	0,152	0,077	0,441	0,225	0,317	0,045	0,000	0,054	na	na
Internal-External rotation	FE	Implant 1 - Implant 2	0,155	0,119	0,037	0,070	0,058	0,079	0,159	0,177	0,184	0,307	0,407	0,047
		Implant 1 - Implant 3	0,023	0,063	0,052	0,061	0,070	0,470	0,222	0,491	0,718	0,531	0,332	0,819
		Implant 2 - Implant 3	1,000	1,000	1,000	1,000	1,000	1,000	1,000	1,000	1,000	1,000	1,000	1,000
	SQ	Implant 1 - Implant 2	1,000	0,004	0,003	0,002	0,000	0,001	0,000	0,000	0,000	0,002	0,092	na
		Implant 1 - Implant 3	1,000	0,201	0,080	0,086	0,019	0,017	0,001	0,001	0,000	0,001	0,181	na
		Implant 2 - Implant 3	0,760	0,250	0,485	0,379	0,359	0,556	0,817	1,000	1,000	1,000	1,000	na
	CH	Implant 1 - Implant 2	0,063	0,008	0,009	0,016	0,009	0,014	0,015	0,016	0,346	0,302	na	na
		Implant 1 - Implant 3	0,008	0,002	0,001	0,001	0,001	0,001	0,001	0,001	0,165	1,000	na	na
		Implant 2 - Implant 3	1,000	1,000	0,928	0,766	1,000	0,814	0,999	0,800	1,000	0,947	na	na

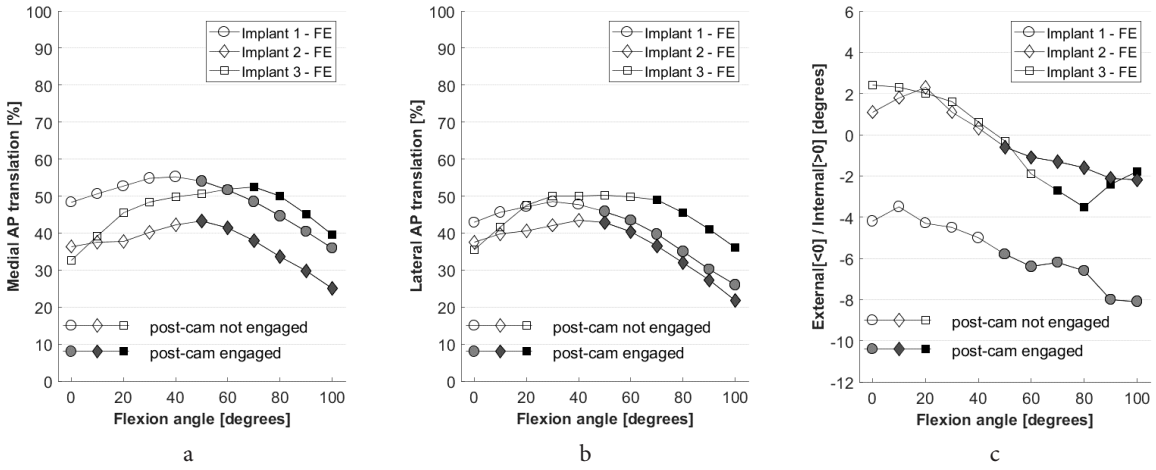

Fig. 2 — Effect of implant type on the anteroposterior position (medial (A) and lateral (B)) and internal-external rotation (C) during open chain flexion-extension movement.

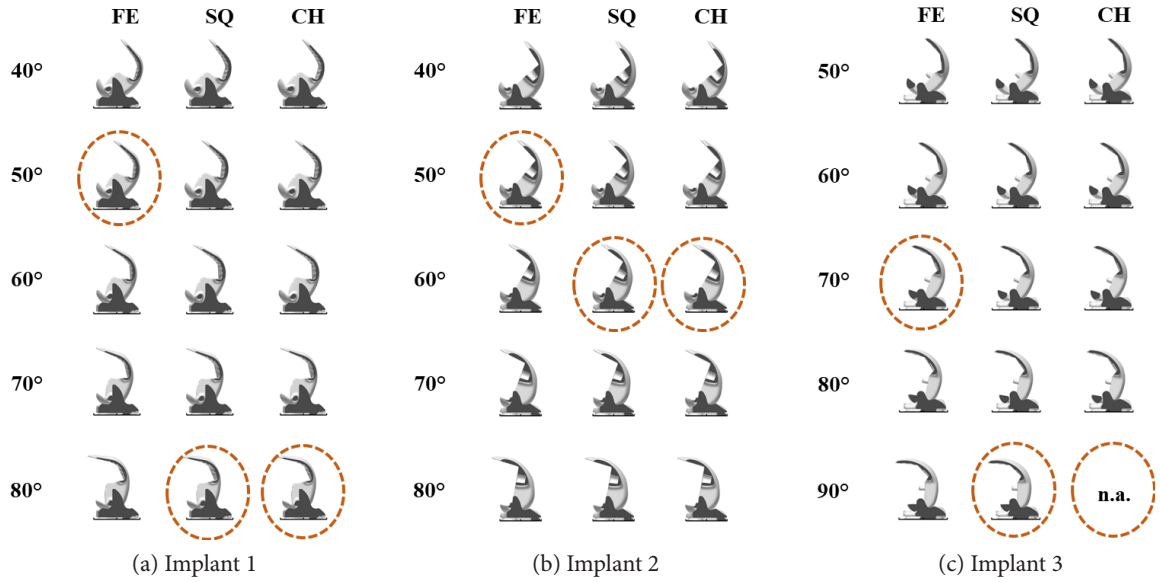

Fig. 3 — Post-cam engagement for different implants through the range of motion during different activities. The moment of post-cam engagement is indicated by the circle.

points method, demonstrated a robust and statistically significant correlation (Pearson correlation coefficient of 0.8066, $p<0.001$). A linear model was applied to the collected data points, incorporating all implants, performed activities, and flexion angles. The model revealed an intercept of 9.565 and a slope of 0.764, represented by the solid line in Figure 5. A standard deviation of 4.89% was observed in the normalized anteroposterior translation, as illustrated by the dotted lines in Figure 5. The chair test in implant 2 demonstrated the most substantial difference between the two measuring methods for the anteroposterior translation. As the flexion decreased towards extension, the lateral contact points exhibited a rapid anterior movement, whereas the landmark utilized in the GS method remained relatively stationary (resulting in a difference of 27.47% and 1.17% for the GS and CP methods, respectively, as illustrated in Figure 6).

DISCUSSION

The most important finding of this study was that the implant design, the performed activity and the used analytical method all affect the in-vivo knee kinematics of posteriorly stabilized knee prostheses. Consequently, the interpretation of fluoroscopic data should be approached with caution, considering the impact of these factors.

Firstly, the results show that implant design affects tibiofemoral kinematics. For AP translation, the differences are more pronounced in the medial

Table III. — Overview of the statistical difference in the anteroposterior position between the listed activities through the range of motion, shown for a given implant. The data are shown separately for the medial and the lateral compartments. The black values are indicative of a p-value less than 0.05.

degrees of flexion			0	10	20	30	40	50	60	70	80	90	100	110
medial AP movement	Implant 1	FE - SQ	0,690	0,658	1,000	0,331	0,021	0,013	0,028	0,273	1,000	1,000	1,000	na
		FE - CH	1,000	1,000	0,417	0,058	0,005	0,005	0,011	0,288	1,000	1,000	1,000	na
		SQ - CH	0,789	0,481	1,000	1,000	1,000	1,000	1,000	1,000	1,000	1,000	1,000	na
	Implant 2	FE - SQ	1,000	0,862	0,355	0,017	0,002	0,002	0,121	0,985	1,000	1,000	na	na
		FE - CH	1,000	1,000	1,000	1,000	0,201	0,092	1,000	1,000	1,000	0,743	na	na
		SQ - CH	1,000	0,511	0,130	0,091	0,140	0,292	0,607	0,312	0,469	1,000	na	na
	Implant 3	FE - SQ	1,000	0,595	1,000	0,398	0,321	0,025	0,003	0,000	0,000	0,107	na	na
		FE - CH	1,000	1,000	1,000	0,392	0,590	0,010	0,002	0,000	0,001	1,000	na	na
		SQ - CH	1,000	1,000	1,000	1,000	1,000	1,000	1,000	1,000	1,000	0,790	na	na
lateral AP movement	Implant 1	FE - SQ	0,043	1,000	0,773	0,297	0,061	0,022	0,015	0,029	0,330	1,000	1,000	na
		FE - CH	1,000	1,000	0,349	0,068	0,022	0,009	0,008	0,038	1,000	1,000	1,000	na
		SQ - CH	0,058	1,000	1,000	1,000	1,000	1,000	1,000	1,000	0,556	1,000	1,000	na
	Implant 2	FE - SQ	1,000	0,465	1,000	1,000	1,000	1,000	1,000	1,000	1,000	1,000	na	na
		FE - CH	1,000	1,000	1,000	0,213	0,079	0,056	0,204	1,000	1,000	1,000	na	na
		SQ - CH	1,000	0,258	0,420	0,440	0,498	0,464	0,310	0,518	0,446	1,000	na	na
	Implant 3	FE - SQ	1,000	1,000	1,000	0,084	0,067	0,004	0,001	0,000	0,018	1,000	na	na
		FE - CH	1,000	1,000	1,000	0,306	0,011	0,006	0,001	0,000	0,005	0,722	na	na
		SQ - CH	0,819	1,000	1,000	1,000	1,000	1,000	1,000	1,000	1,000	0,531	na	na
Internal-External rotation	Implant 1	FE - SQ	0,308	1,000	1,000	1,000	1,000	0,995	0,579	0,655	0,656	1,000	1,000	na
		FE - CH	1,000	1,000	0,913	0,801	0,860	0,809	0,566	0,720	1,000	1,000	1,000	na
		SQ - CH	0,305	1,000	1,000	1,000	1,000	1,000	1,000	1,000	0,874	1,000	1,000	na
	Implant 2	FE - SQ	1,000	0,398	0,762	0,740	0,769	0,820	0,977	1,000	1,000	1,000	na	na
		FE - CH	1,000	1,000	1,000	1,000	1,000	1,000	1,000	1,000	1,000	1,000	na	na
		SQ - CH	1,000	0,200	0,161	0,148	0,146	0,216	0,262	0,280	0,337	1,000	na	na
	Implant 3	FE - SQ	0,596	0,869	1,000	1,000	1,000	1,000	1,000	0,483	0,313	0,313	na	na
		FE - CH	1,000	1,000	1,000	1,000	1,000	1,000	1,000	1,000	1,000	1,000	na	na
		SQ - CH	0,268	1,000	1,000	1,000	1,000	1,000	1,000	1,000	0,801	0,270	na	na

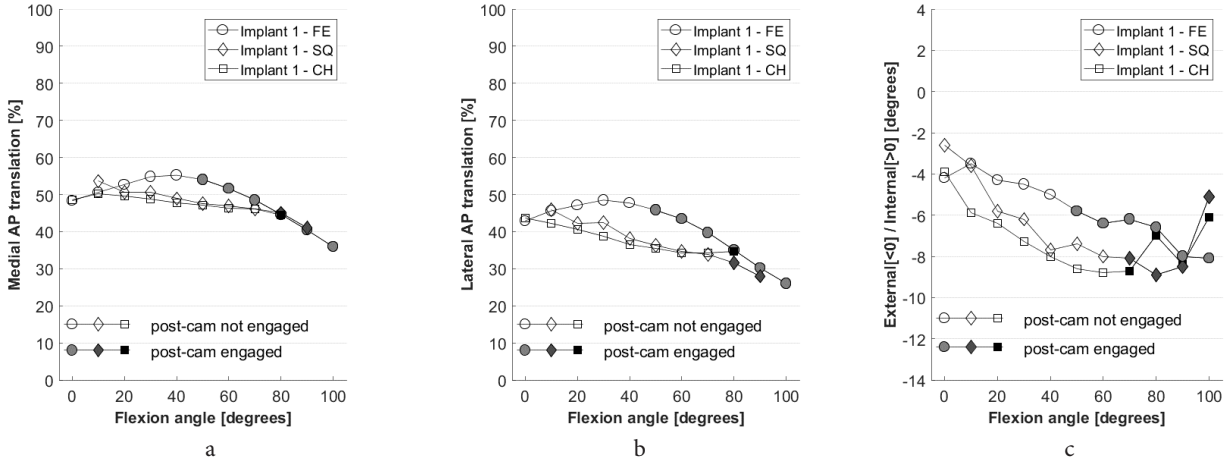

Fig. 4 — Medial (a) and lateral (b) normalized anteroposterior position and internal-external rotation through the range of motion for implant 1, shown by performed activity.

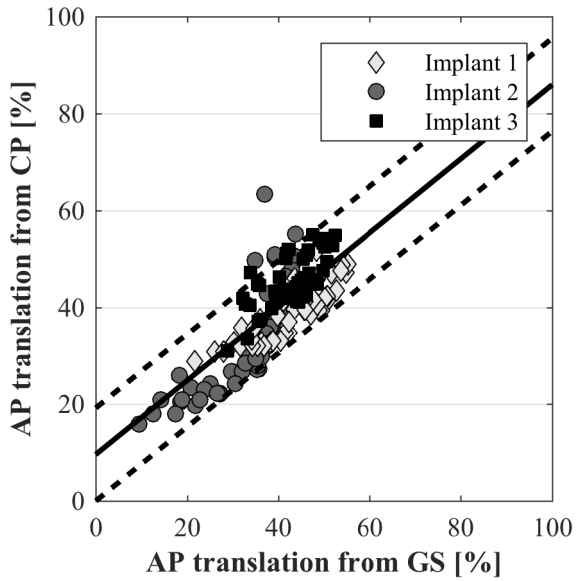

Fig. 5 — Correlation between the kinematics from the contact points method and the landmark-based method.

compartment (Table I). This can be most likely attributed to the relationship between the knee kinematics and the implant geometry at the medial side. In general, stability is primarily enhanced through the design of the medial compartment, such as incorporating a deeper dish in the medial insert. Given that different implants may be developed based on varying design hypotheses, variations in anteroposterior kinematics are expected. Conversely, the lateral compartment is characterized by less constraint and therefore has less impact on the kinematics when performing the same activity. Clearly, it should be noted that this holds true until the post-cam engagement. From that point on, further movement is restricted by the implant design.

The moment of post-cam engagement is based on the implant characteristics and consequently differs among the different implants. As the flexion angle increases, implant 2 exhibited the earliest engagement of its post-cam mechanism, followed by implant 1 and then implant 3. Therefore, the timing of post-cam engagement plays a crucial role in the anteroposterior translation in all the implants.

The moment of engagement corresponds to the initiation of a pronounced and controlled posterior translation, defined as the femoral rollback. Given the later engagement in implant 3, the tibiofemoral position is situated more anteriorly during deeper flexion. In contrast, at these flexion angles, the post-cam has already been engaged in the other implants, leading to a more posterior position.

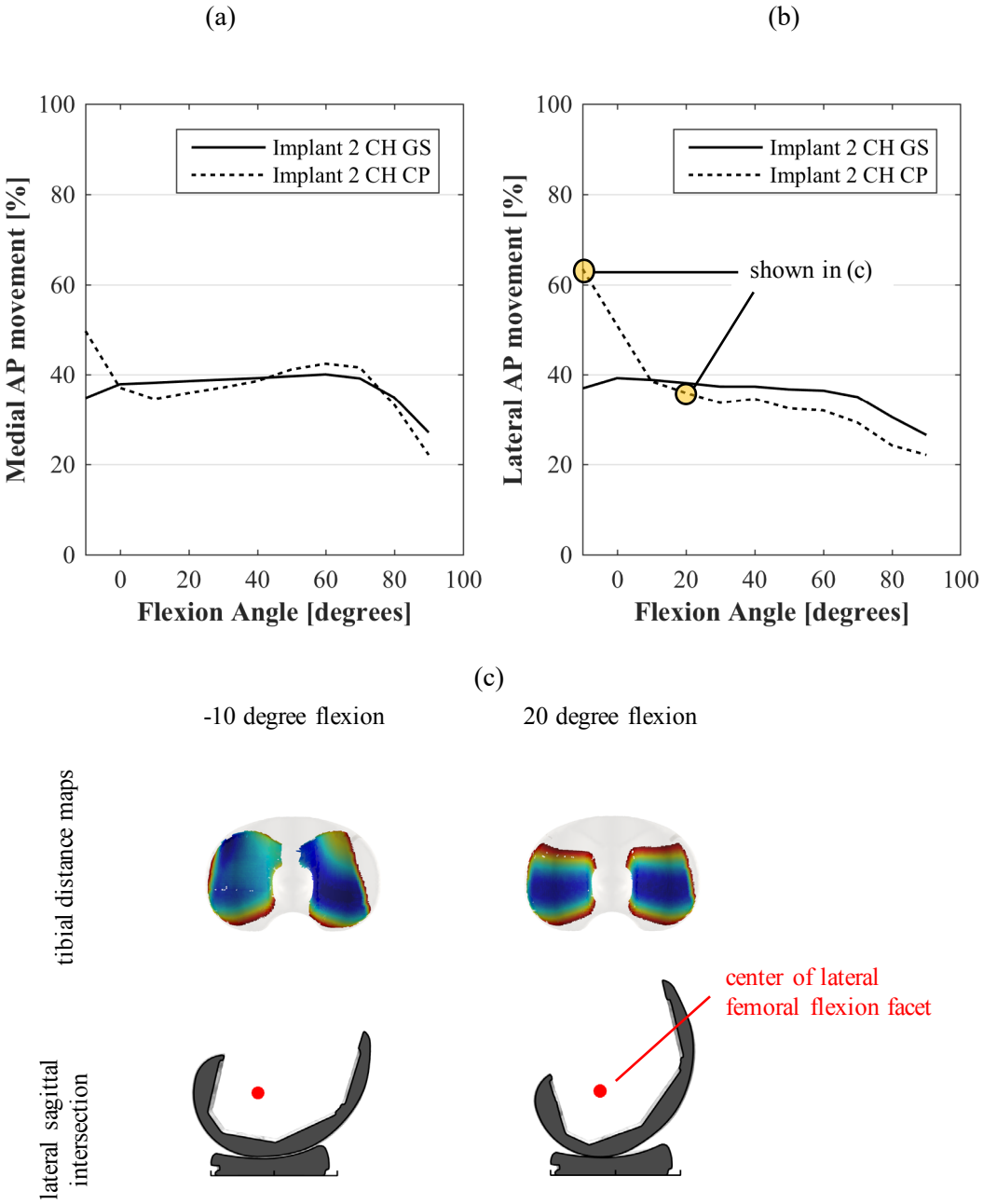

Fig. 6 — Overview of anteroposterior translation for the medial (a) and lateral (b) compartment for implant 2, shown by analytical method. (c) Distance maps indicating the effect of small translation of lateral femoral condylar center (-1.17% / GS) on shift of contact points (-27.47% / CP) for a highly conform implant (implant 2).

More specifically, engagement typically occurs between 50 and 90 degrees of flexion. This observed variation corresponds to the results published earlier[4,6]. The moment of engagement is directly associated with the positioning of both the post and the cam components (Figure 7). Implant 2 has a more posterior placement of the post, and thereby leading to an earlier engagement. Conversely, implant 3 has a delayed engagement attributed to the anterior position of the post in combination with the elevated position of the cam. Implant 1 represents an intermediate scenario between implants 2 and 3.

Secondly, the activity performed affects the observed tibiofemoral kinematics. The activities investigated in this study can be categorized into two groups: open chain (flexion-extension) and closed chain (squatting and chair rising), characterized by weight bearing. The medial and lateral anteroposterior positions were not significantly different between both closed chain activities. On the other hand, a difference in kinematics is observed between open and closed chain activities, specifically in mid-flexion. During

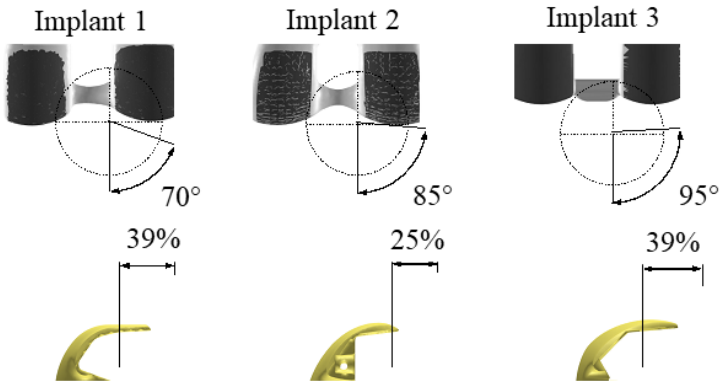

Fig. 7 — Overview of post-cam positioning in the different implants of this study. The bottom shows the posterior placement of the post. The top shows the different geometry.

this range of motion, the closed chain activities lead to a more posterior positioning of the components in both compartments, which is consistent with the findings reported by Shimizu and colleagues[9]. Biomechanically, the posterior position increases the patella lever arm of the extensor mechanism, to address the higher requirements of closed-chain exercises[18]. Insight into the tibiofemoral shear forces and patellofemoral contact forces in intact, healthy knees provided by the work of Smidt and Dahlkvist helps to understand this observed difference[19,20]. Closed-chain activities are associated with higher forces compared to open chain activities, thereby possibly pushing the femur more posteriorly relative to the tibia. However, it should be noted that our analyses only identified differences in the mid-flexion range. Nevertheless, this can be attributed to the specific characteristics of the posteriorly stabilized total knee implants examined within our study population. Near extension, knee kinematics are determined by the congruency between the tibial and femoral components. For example, implant 1 is designed to prevent posterior femoral overhang in full extension. Moreover, the design of the implant withhold the anteroposterior translation of the compartments, minimizing the influence of external forces on the joint. Likewise, the knee kinematics in deep flexion are determined by the post-cam engagement, leading to the absence of significant differences in that position between the activities. As earlier described, closed chain activities are associated with a more posterior tibiofemoral position. This postpones the post-cam engagement compared to the open chain activities. This is primarily described for implants 1 and 3 and less for implant 2. This can be due to the combination of a relative early post-cam engagement and a single radius design of implant 2, which maintains the tibiofemoral congruency with increasing flexion angles.

Thirdly, the applied analytic method also affects the reported kinematics. To the best of our knowledge, this is the first study that compares the contact points method and the landmark-based method. Using the contact points is considered to offer a more comprehensive understanding of the actual implant design, as it explicitly incorporates the geometry and conformity of the components. Consequently, significant shifts in the location of the contact points can be observed even with minimal rotations and translations of the components, potentially emphasizing the significance of design characteristics, like the shape of the insert. However, our study revealed that this analysis method is sensitive to slight variations in the conversion from 2D to 3D. Nevertheless, the accuracy of our single-plane fluoroscopy aligns with previous findings reported in the literature[21,22]. Individually, this method is less useful. However, this method provided valuable information when investigating the kinematics of a specific movement within a cohort of patients with same implant. In contrast, the landmark-based method, which is independent of implant conformity, seems to be more pertinent for assessing the movement of the bone segments. This alternative method provides valuable insights into the loads transferred to the soft tissue envelop, encompassing both interacting segments. Moreover, it is less susceptible to inaccuracies stemming from the 2D-3D conversion process, as it allows for separate evaluation of the joint kinematics in different degrees of flexion. Therefore, the use of the landmark-based method to evaluate out-of-plane translations is not recommended. In contrast, for in-plane translations, this method is reliable. Both the contact points method and the landmark-based method shows a strong correlation. However, a notable standard deviation of 25% was observed for anteroposterior translation. This

variability is influenced by various factors, including implant design, such as the level of conformity between articulating surfaces, as well as activity-related factors, such as presence of shear load and the magnitude. In recent years, there has been increased focus on the conformity of implants, particularly regarding the utilization of medial pivot implants or medial constraint polyethylene inserts in conventional cruciate retaining and/or posteriorly stabilized implants. Since a single implant can accommodate different types of inserts, it is recommended to use the contact points as a reference to define the kinematics. Generally, both methods are not interchangeable but rather serve as complementary approaches to describe kinematics. Therefore, results should be interpreted considering the specific method applied.

This study is highly significant as it illuminates several crucial factors that influence knee kinematics, particularly concerning a posterior stabilized design. While outcome measures like PROMs typically provide consistent and user-friendly data, there is considerable variation in the methods and analyses employed in fluoroscopy, a pivotal tool for assessing kinematics. By detailing the methodology used in this evaluation, the study not only provides insights into the specific technique employed but also into the subsequent analytical approaches. Moreover, this study presents a valuable overview of three key factors influencing knee kinematics, thereby advancing understanding and knowledge in this field.This study has several limitations. Firstly, the comparison between different implants is hindered by challenges in identifying landmarks. Both the fitting of the spheres and the relative anteroposterior position have their inherent limitations. To mitigate this issue, elastic, non-rigid deformation algorithms were employed to optimally match the flexion facets between different implant designs and sizes. These algorithms used detailed 3D CAD files to accurately transfer the area between implants. Secondly, it is important to note that the factors influencing tibiofemoral kinematics, as reported in this study, are not exclusive and may be influenced by additional variables.

CONCLUSIONS

This study described the effect of the implant design, performed activity and used analytical method on the in-vivo knee kinematics of posteriorly stabilized knee prostheses. Firstly, the implant type, as characterized by the geometry and the post-cam mechanism, determines the anteroposterior position of the implant. The differences between three modern posteriorly stabilized knee prosthesis are primarily located in the medial compartment. Secondly, the performed activity significantly impacts the tibiofemoral kinematics. Particularly, the kinematic pattern proceeds differently for closed chain than for open chain activities during mid-flexion. Furthermore, closed chain activities are associated with a delayed post-cam engagement. A third factor crucial to consider, is the analytical method used in a kinematic study based on fluoroscopic data. In our study, a strong correlation is observed between the landmark-based and the contact points method, although not uniquely linked to each other. The landmark-based focuses solely on the bone movements, while the contact points also accounts for the conformity of the components. Therefore, the importance of the contact points method will grow in the future given the availability of different inserts for one type of implant.

REFERENCES

1. Dessinger GM, LaCour MT, Dennis DA, et al (2021) Can an OA Knee Brace Effectively Offload the Medial Condyle? An In Vivo Fluoroscopic Study. J Arthroplasty 36:1455–1461. https://doi.org/10.1016/j.arth.2020.10.044
2. Michael Johnson J, Mahfouz MR (2016) Cartilage loss patterns within femorotibial contact regions during deep knee bend. J Biomech 49:1794–1801. https://doi.org/10.1016/j.jbiomech.2016.04.011
3. Palm-Vlasak LS, Smith J, Harvey A, et al (2023) Posterior cruciate-retaining total knee arthroplasty exhibits small kinematic changes in the first postoperative year. Knee Surgery, Sports Traumatology, Arthroscopy 31:914–921. https://doi.org/10.1007/s00167-022-07027-x
4. Arnout N, Vanlommel L, Vanlommel J, et al (2015) Post-cam mechanics and tibiofemoral kinematics: a dynamic in vitro analysis of eight posterior-stabilized total knee designs. Knee Surgery, Sports Traumatology, Arthroscopy 23:3343–3353. https://doi.org/10.1007/s00167-014-3167-2
5. Fitzpatrick CK, Clary CW, Cyr AJ, et al (2013) Mechanics of post-cam engagement during simulated dynamic activity. Journal of Orthopaedic Research 31:1438–1446. https://doi.org/10.1002/jor.22366
6. Mihalko WM, Lowell J, Higgs G, Kurtz S (2016) Total Knee Post-Cam Design Variations and Their Effects on Kinematics and Wear Patterns. Orthopedics 39:. https://doi.org/10.3928/01477447-20160509-14
7. Zingde SM, Leszko F, Sharma A, et al (2014) In Vivo Determination of Cam-Post Engagement in Fixed and Mobile-bearing TKA. Clin Orthop Relat Res 472:254–262. https://doi.org/10.1007/s11999-013-3257-3
8. Victor J, Labey L, Wong P, et al (2009) The influence of muscle load on tibiofemoral knee kinematics. Journal of Orthopaedic Research n/a-n/a. https://doi.org/10.1002/jor.21019
9. Shimizu N, Tomita T, Yamazaki T, et al (2011) The Effect of Weight-Bearing Condition on Kinematics of a High-Flexion, Posterior-Stabilized Knee Prosthesis. J Arthroplasty 26:1031–1037. https://doi.org/10.1016/j.arth.2011.01.008
10. Victor J, Banks S, Bellemans J (2005) Kinematics of posterior cruciate ligament-retaining and -substituting total knee

arthroplasty. J Bone Joint Surg Br 87-B:646–655. https://doi.org/10.1302/0301-620X.87B5.15602
11. Wolterbeek N, Garling EH, Mertens BJA, et al (2012) Kinematics of a highly congruent mobile-bearing total knee prosthesis. Knee Surgery, Sports Traumatology, Arthroscopy 20:2487–2493. https://doi.org/10.1007/s00167-012-1936-3
12. Luyckx T, Peeters T, Vandenneucker H, et al (2012) Is adapted measured resection superior to gap-balancing in determining femoral component rotation in total knee replacement? J Bone Joint Surg Br 94:1271–1277. https://doi.org/10.1302/0301-620X.94B9
13. Van Onsem S, Verstraete M, Van Eenoo W, et al (2020) Are TKA Kinematics During Closed Kinetic Chain Exercises Associated with Patient-reported Outcomes? A Preliminary Analysis. Clin Orthop Relat Res 478:255–263. https://doi.org/10.1097/CORR.0000000000000991
14. Daems R, Victor J, De Baets P, et al (2016) Validation of three-dimensional total knee replacement kinematics measurement using single-plane fluoroscopy. International Journal Sustainable Construction & Design 7:14. https://doi.org/10.21825/scad.v7i1.3634
15. Grood ES, Suntay WJ (1983) A Joint Coordinate System for the Clinical Description of Three-Dimensional Motions: Application to the Knee. J Biomech Eng 105:136–144. https://doi.org/10.1115/1.3138397
16. Farrokhi S, Voycheck CA, Gustafson JA, et al (2016) Knee joint contact mechanics during downhill gait and its relationship with varus/valgus motion and muscle strength in patients with knee osteoarthritis. Knee 23:49–56. https://doi.org/10.1016/j.knee.2015.07.011
17. Hosseini Nasab SH, Smith CR, Schütz P, et al (2019) Elongation Patterns of the Collateral Ligaments After Total Knee Arthroplasty Are Dominated by the Knee Flexion Angle. Front Bioeng Biotechnol 7:. https://doi.org/10.3389/fbioe.2019.00323
18. Grelsamer RP, Weinstein CH (2001) Applied Biomechanics of the Patella. Clin Orthop Relat Res 389:9–14. https://doi.org/10.1097/00003086-200108000-00003
19. Dahlkvist NJ, Mayo P, Seedhom BB (1982) Forces during Squatting and Rising from a Deep Squat. Eng Med 11:69–76. https://doi.org/10.1243/EMED_JOUR_1982_011_019_02
20. Smidt GL (1973) Biomechanical analysis of knee flexion and extension. J Biomech 6:79–92. https://doi.org/10.1016/0021-9290(73)90040-7
21. Banks SA, Hodge WA (1996) Accurate measurement of three-dimensional knee replacement kinematics using single-plane fluoroscopy. IEEE Trans Biomed Eng 43:638–649. https://doi.org/10.1109/10.495283
22. Mahfouz MR, Hoff WA, Komistek RD, Dennis DA (2003) A robust method for registration of three-dimensional knee implant models to two-dimensional fluoroscopy images. IEEE Trans Med Imaging 22:1561–1574. https://doi.org/10.1109/TMI.2003.820027